Structural basis of DNA crossover capture by Escherichia coli DNA gyrase

Marlène Vayssières, Nils Marechal, Long Yun, Brian Lopez Duran, Naveen Kumar Murugasamy, Jonathan Fogg, Lynn Zechiedrich, Marc Nadal, Valérie Lamour

HHS Public Access

Author manuscript

Science. Author manuscript; available in PMC 2024 May 21.

Published in final edited form as:

Science. 2024 April 12; 384(6692): 227–232. doi:10.1126/science.adl5899.

Structural basis of DNA crossover capture by *Escherichia coli* DNA gyrase

Marlène Vayssières[1,2], **Nils Marechal**[1,2], **Long Yun**[3], **Brian Lopez Duran**[1,2], **Naveen Kumar Murugasamy**[1,2], **Jonathan M. Fogg**[4,5], **Lynn Zechiedrich**[4,5], **Marc Nadal**[3,4,6,*], **Valérie Lamour**[1,2,7,*]

[1]Université de Strasbourg, Centre National de la Recherche Scientifique (CNRS), Institut national de la Recherche Médicale (INSERM), Institut de Génétique et de Biologie Moléculaire et Cellulaire (IGBMC), UMR 7104- UMR-S 1258, F-67400 Illkirch, France.

[2]Department of Integrated Structural Biology, IGBMC, Illkirch, France.

[3]Institut de Biologie de l'Ecole Normale Supérieure (IBENS), École normale supérieure, CNRS, INSERM, Université PSL, Paris, France.

[4]Department of Molecular Virology and Microbiology, Baylor College of Medicine, Houston, TX, USA.

[5]Verna and Marrs McLean Department of Biochemistry and Pharmacology, Baylor College of Medicine, Houston, TX, USA.

[6]Department of Life Sciences, Université Paris Cité, Paris, France.

[7]Hôpitaux Universitaires de Strasbourg, Strasbourg, France.

Abstract

DNA supercoiling must be precisely regulated by topoisomerases to prevent DNA entanglement. The interaction of type IIA DNA topoisomerases with two DNA molecules, enabling the transport of one duplex through the transient double-stranded break of the other, remains elusive owing to structures derived solely from single linear duplex DNAs lacking topological constraints. Using cryo–electron microscopy, we solved the structure of *Escherichia coli* DNA gyrase bound to a

[*]**Corresponding author.** lamourv@igbmc.fr (V.L.); manadal@bio.ens.psl.eu (M.N.).

Author contributions: Conceptualization: J.M. F., L.Z., M.N., and V.L. Methodology: N.M., J.M.F., L.Z., M.N., and V.L. Investigation: M.V., N.M., L.Y., B.L.D., N.K.M., M.N., and V.L. Visualization: M.V., N.M., M.N., and V.L. Funding acquisition: L.Z., M.N., and V.L. Project administration: V.L. Supervision: M.N. and V.L. Writing – original draft: M.V., N.M., M.N., and V.L. Writing – review and editing: M.V., N.M., N.K.M., B.L.D., J.M.F., L.Z., M.N., and V.L.

Competing interests: J.M.F. and L.Z. hold equity in Twister Biotech. The authors declare no other competing interests.

SUPPLEMENTARY MATERIALS

science.org/doi/10.1126/science.adl5899

Materials and Methods

Figs. S1 to S13

Tables S1 and S2

References (51–77)

Movie S1

Data S1 to S5

MDAR Reroducibility Checklist

negatively supercoiled minicircle DNA. We show how DNA gyrase captures a DNA crossover, revealing both conserved molecular grooves that accommodate the DNA helices. Together with molecular tweezer experiments, the structure shows that the DNA crossover is of positive chirality, reconciling the binding step of gyrase-mediated DNA relaxation and supercoiling in a single structure.

For most organisms, DNA adopts a state of negative supercoiling [(−)SC], a condition known to promote unwinding of the DNA helix, facilitating access to genetic information for the molecular machinery involved in critical cellular processes (1). By contrast, positive supercoiling [(+)SC] is generated ahead of the DNA replication and transcription machinery (2). In the absence of topoisomerases that relax (+)SC, these fundamental processes become hindered (3). The type IIA DNA topoisomerases (TopoIIA) are evolutionarily conserved macromolecules that modulate DNA topology by transporting a DNA duplex through a transient double-strand break, enabling DNA relaxation, decatenation, and unknotting (4). TopoIIA enzymes are major targets for therapeutics used for infectious diseases and cancer treatments (5, 6).

Supercoiled DNA can adopt a broad range of possible conformations (7–10). How topoisomerases recognize such a structurally diverse molecule has been the subject of much debate. TopoIIA preferentially binds DNA crossovers (nodes) or DNA-DNA juxtapositions (11). Were TopoIIA to act indiscriminately at every DNA juxtaposition, increased entanglement would result, which would be potentially disastrous for the cell (12). How TopoIIA enzymes recognize DNA crossovers that indicate a problematic entanglement requiring resolution is a question that has fueled numerous models (13–16).

Structural studies of the full-length bacterial DNA gyrase, yeast Topo II, and the human enzyme (hTopoIIa) have revealed the evolutionarily conserved quaternary organization of these modular enzymes (17–19). The TopoIIA catalytic core consists of three dimer interfaces called the N-gate, the DNA-gate, and the C-gate. The enzymes exhibit conformational flexibility and allostery to regulate these interfaces, facilitating DNA binding, cleavage, and strand passage through ATP hydrolysis (figs. S1A and S2) (4, 20). The structural diversity among TopoIIA subtypes across various organisms is predominantly found within the C-terminal domain (CTD), which is thought to contribute to DNA binding and sensing of DNA topology (21–24). The CTD of DNA gyrase exhibits a distinctive β-pinwheel domain that is essential for the ability of the enzyme to introduce (−)SC into DNA (25–27).

It was long ago hypothesized that DNA gyrase could introduce negative supercoils by first wrapping DNA to form a transient (+)SC DNA crossover (28). Gyrase-mediated passage of one of the crossover helices, named the T-segment for transport, through the other, called the gate or G-segment, converts the (+)SC to a (−)SC crossover, thus causing a sign inversion (fig. S1, B and C). Previous molecular structures of TopoIIA enzymes were obtained bound to short linear duplex DNA, the G-segment only, and in a completely closed conformation of the protein gates (17–19). Consequently, how the enzymes recognize the T-segment of DNA is unknown.

In this study, we report high-resolution cryo–electron microscopy (cryo-EM) structures of *Escherichia coli* DNA gyrase bound on a (−)SC DNA minicircle at a DNA crossover. Our reconstruction of the complex reveals that at the binding step, the adenosine triphosphatase (ATPase) domain of gyrase is completely open. The structure coupled with single-molecule experiments unveil, just as proposed 44 years ago, that the enzyme captures and stabilizes a positive DNA crossover, supporting the sign-inversion mechanism (28). Our structure reveals how a DNA crossover is recognized by the enzyme, with the G- and T-segment double helices shielded from each other and embedded in conserved protein grooves of TopoIIA. Our reconstruction also shows how the C-terminal β-pinwheel domain enables the capture of a (+)SC DNA crossover in a molecule that is overall (−)SC.

Results

Cryo-EM structures of E. coli DNA gyrase bound to negatively supercoiled DNA minicircles

We first formed a complex between the wild-type (WT) and active *E. coli* DNA gyrase (A_2B_2) heterotetramer, purified as in (18), and a (−)SC DNA minicircle of 601 base pairs (bp) with a change in linking number (ΔLk) of −1 prepared by using a protocol derived from (9, 29) (fig. S3A), but we saw no gyrase-minicircle complexes. To prevent DNA relaxation and dissociation of the complex, we used an inactive $A^{(Y122F)}{}_2B_2$ heterotetramer in which the catalytic tyrosine was mutated to phenylalanine. We also increased the negative supercoiling in the minicircles to $\Delta Lk = -2$. To verify the *Lk*, we relaxed this minicircle with either a type I *E. coli* topoisomerase 1 (*Ec*Top1) that relaxes (−)SC in *Lk* steps of one, or the type IIA enzyme, hTopoIIα, that relaxes *Lk* in steps of two (Fig. 1A). As expected, EcTop1 partially relaxed the $\Delta Lk = -2$ substrate to $\Delta Lk = -1$. Relaxation with hTopoIIα yielded only relaxed DNA ($\Delta Lk = 0$), confirming the *Lk* designation of the substrate.

We immobilized the minicircle-gyrase complexes on streptavidin affinity grids (SAGs) using the $\Delta Lk = -2$ minicircle, containing one biotinylated nucleotide, incubated with a 20-fold excess of the mutant gyrase and adenylyl-imidodi-phosphate (AMP-PNP) (Fig. 1B and fig. S3B) (30). Two datasets of the complex were collected on a transmission cryo–electron microscope leading to two high-resolution three-dimensional (3D) reconstructions (Fig. 1C, figs. S4 and S5, and table S1).

One reconstruction (at 3.0 Å resolution) was the most abundant particle observed: gyrase on a DNA crossover formed between contiguous DNA T- and G-segments encompassing 118 bp (Fig. 2, A and B). The DNA was wrapped around one of the C-terminal β-pinwheel domains, and the ATPase domains were completely open (Fig. 2). The other 3D reconstruction was gyrase on a linear part of the DNA minicircle (at 2.9 Å resolution) (figs. S4, S5, and S6A). This structure had less well-defined density for both β-pinwheel domains, suggesting higher flexibility of this region than when bound to the DNA crossover.

The catalytic core of gyrase, composed of the ATPase and DNA binding-cleavage domains, are superimposable between the two 3D reconstructed conformations with a 0.23 Å root mean square deviation (RMSD) over all residues (Fig. 2 and fig. S6, A and B). The dimeric conformation of the DNA binding-cleavage domain upon DNA crossover binding is reminiscent of a precleavage conformational state observed in previous crystal structures

(1.4 Å RMSD over all residues) (fig. S6D), with a similarly bent G-segment DNA (figs. S6F and S7, A and B) (17, 18, 31, 32).

Despite the presence of AMP-PNP in our sample, which we expected to "lock" the enzyme at the N-gate, the ATPase domains of the GyrB subunit were opened and positioned adjacent to the remainder of the enzyme core in both reconstructions (Fig. 2 and fig. S6, A to C). The linkers connecting the ATPase domain to the topoisomerase-primase (TOPRIM) domain were also apart from each other on each side of the DNA G-segment, which is in contrast to their crossed position bound to the G-segment DNA only (18).

The ATPase domains interact with the rest of the protein throughout three protein-protein interfaces, mainly involving the TOPRIM domain (fig. S6C). In total, six hydrogen bonds were established with different residues in the TOPRIM domain, and eight were established specifically with the *E. coli* insertion-TOPRIM domain (33).

DNA crossover interactions with gyrase

The reconstruction allowed us to observe the complete wrapping of DNA around a β-pinwheel domain of the gyrase CTD, leading to the formation of an intramolecular DNA crossover (Fig. 2 and fig. S8A). Density for the second CTD could not be observed in the cryo-EM map, indicating that the DNA crossover forms around and stabilizes a single β-pinwheel.

As reported for previousstructures (17, 18, 31,32), the G-segment of the DNA minicircle binds to the main groove of the enzyme DNA-gate formed by the TOPRIM, winged helix domain (WHD), and Tower domains, and with a similar sharp bend as that observed in the complex with only one linear DNA (fig. S6F). We could not obtain the DNA sequence register despite the 2.4 Å local resolution, which indicates that gyrase may bind to multiple different sites.

One of the informative features in the structure is the presence of the DNA T-segment forming a complete DNA crossover of two superposed DNA helices. In contrast to previous structures (18, 24), the presence of the T-segment stabilized the β-pinwheel blades, forming a flat and fully closed disk (fig. S8, B to D) similar to the structure of the isolated GyrA-CTD from *B. burgdorferi* (26). The β-pinwheel domain adopted a new position, tilted by 30° compared with its position in the cryo-EM structure of *E. coli* DNA gyrase alone (fig. S8E) (18). DNA wrapping is enforced by interactions with the GyrA-box motif within blade 1 of the CTD β-pinwheel. The basic residues R561, R562, and K565 of the GyrA-box intercalate into successive grooves of the T-segment and, together with additional major groove interactions of R613 and R615 from blade 2, stabilize an overall 360° DNA wrap (fig. S8A). Because of the single-particle approach and the presence of the streptavidin crystal array, the rest of the DNA minicircle beyond the gyrase binding sites could not be observed. [Single-letter abbreviations for the amino acid residues are as follows: A, Ala; C, Cys; D, Asp; E, Glu; F, Phe; G, Gly; H, His; I, Ile; K, Lys; L, Leu; M, Met; N, Asn; P, Pro; Q, Gln; R, Arg; S, Ser; T, Thr; V, Val; W, Trp; and Y, Tyr.]

The β-pinwheel domain of gyrase is positioned to orient the T-segment in a second groove of the DNA-gate formed by the TOPRIM, WHD, and Tower domains, directly above the DNA-gate (fig. S11A). The T-segment interacts through positively charged residues stabilized by acidic residues with four protein regions: the β-pinwheel, the linker between the transducer and TOPRIM domains, the lysine-rich loop ("K-loop") of the transducer domain, and loop regions in the tower domain (Fig. 3A and fig. S8). In contrast to the yeast structure, the K-loop is contacting the T-segment, instead of the G-segment as seen in the yeast structure (17). As a result, the full length of the T-segment is sitting at the protein dimeric interface, with a slight (~160°) bending in the middle of the T-segment, with fewer protein contacts (Fig. 2C). The G- and T-segments intersect at a 60° angle, as previously anticipated from structures with longer linear DNA (18, 34). The DNA segments, however, do not sit directly on top of each other as commonly represented in schematics of the catalytic cycle of TopoIIA enzymes. Instead, they are shielded by protein residues. Consequently, they are vertically separated by an average of ~20 Å, ranging from ~25 Å when exiting the β-pinwheel to a minimum distance of ~17 Å on the opposite side (Fig. 2C).

Chirality of the DNA crossover

Another feature of the structure is that the geometry of the enzyme-binding grooves imposes the formation of a positive supercoil, even against the topological torsion from the (−)SC DNA minicircle (Fig. 3B). To verify this observation, we assessed the chirality using magnetic tweezers. A linear DNA was tethered to a magnetic bead with controllable rotation and force at one end and to a glass surface at the other. The bead position was monitored to determine the DNA end-to-end extension of the DNA, which changes with supercoiling (35).

If gyrase constrains a positive wrap in the (−)SC DNA, an additional negative supercoil must be formed elsewhere in the DNA, thus decreasing the DNA extension (Fig. 4A). Upon addition of the catalytically inactive [$A^{(Y122F)}{}_2B_2$] gyrase to (−)SC DNA, by using buffer conditions similar to those used for cryo-EM, the extension was reduced by an average of 75 nm (Fig. 4B), which is equivalent to the bead extension decrease observed upon the addition of 1.25 negative supercoils in a calibration experiment (fig. S9). As a comparison, we performed a similar experiment with (+)SC DNA. Upon DNA binding to an already existing positive node, the β-pinwheel should wrap and tighten the positive supercoil and release excess DNA length, therefore resulting in an increase in DNA extension (Fig. 4C). After addition of the mutant gyrase to (+)SC DNA, we observed an ~75 nm increase in DNA extension, which is consistent with the release of about 1.25 supercoils (Fig. 4D and fig. S9). Altogether, these experiments suggest that DNA gyrase shapes DNA of different chirality in the same manner, by stabilizing a positive crossover (or node), as observed in the cryo-EM structure.

Contribution of the CTD β-pinwheel domain to the catalytic activities of DNA gyrase

To probe the contribution of the gyrase-specific CTD to its catalytic activities, we removed the β-pinwheel domain of the GyrA subunit (ΔCTD). Similar to results for other TopoIIA enzymes and as previously demonstrated for gyrase (23), the mutant gyrase retained the ability to relax (−)SC DNA in the presence of adenosine triphosphate (ATP) (fig. S10B).

This result demonstrates that the CTD of DNA gyrase is not essential for crossover binding or DNA strand passage during the relaxation of negative supercoils.

Unlike the eukaryotic TopoIIA enzymes, which require ATP for effective DNA strand passage activities, full-length gyrase relaxes (−)SC in the absence of ATP in vitro (23). Removal of the CTD incapacitates the ATP-independent relaxation activity of gyrase (fig. S10B) (23). Our data, together with previous results, suggest that stabilization of the T-segment by the CTD β-pinwheel allows strand passage even in the absence of ATP. When the CTD β-pinwheel is absent, and the T-segment is no longer stabilized, dimerization and closure of the ATPase domain upon ATP addition is required for strand passage.

Discussion

Molecular basis of DNA crossover binding by a TopoIIA enzyme

The structural data presented here provide unequivocal evidence for the capture of a DNA crossover by *E. coli* DNA gyrase. Recognition of the DNA crossover is determined primarily by the binding of the T- and G-segments, which are concealed within two protein grooves that our structure unveiled.

DNA wrapping around the CTD to generate a positive crossover appears to be specific to DNA gyrase. The structure reveals how the GyrA-box spatially stabilizes the T-segment in a DNA crossover, highlighting the critical role of this peptidic pattern in “the end of wrap” mechanism that biochemical evidence had suggested (36–38).

The CTDs of the eukaryotic TopoIIA enzymes structurally diverge from the bacterial homologs. The eukaryotic CTDs are predicted to be intrinsically disordered and dispensable for DNA relaxation (19, 39, 40). The conventional TopoIIA DNA relaxation activity observed with ΔCTD gyrase suggests that DNA wrapping around its CTD is responsible for the negative supercoiling and ATP-independent relaxation activities that are specific to gyrase (fig. S10) (23). These activities may require additional interactions provided by the CTD to maintain and transport the T-segment even against any torsional constraints in the DNA substrate.

Other TopoIIA enzymes may use a similar mechanism to bind DNA crossovers. Their amino acid sequence conservation and our modeling of a DNA crossover on the cleavage domain of other TopoIIA enzymes suggest that the T-segment might bind with the same orientation as that for gyrase. Other enzymes have a more positively charged TOPRIM domain than that of gyrase, which perhaps compensates for the absence of pinwheels (figs. S11 and S12). Provided that the orientation of the DNA grooves defines the chirality of the captured DNA node, the fact that other enzymes may have this T-segment groove may explain the preference of some TopoIIA enzymes for binding and relaxing (+)SC over (−)SC DNA (21, 41).

Structural implication of the open conformation upon DNA crossover binding

In our structure, the open conformation of the ATPase GHKL subdomain, which is the region hosting the ATP binding pocket, interacts with the GyrB TOPRIM domain (Figs. 2A

and 3B and fig. S6C). Fluorescence resonance energy transfer (FRET) experiments showed that a catalytically inactive mutant of *Bacillus subtilis* gyrase had an open N-gate, which is consistent with our structural data (42). The ATPase domains of *Mycobacterium tuberculosis* gyrase also were found to be open in a crystal structure but in a higher position (43) than in our structures (fig. S7C). Although the *M. tuberculosis* gyrase conformation was determined in absence of DNA, it is incompatible with the binding of a DNA crossover; it could thus represent a separate intermediate preceding DNA binding.

Recent crystal structures of the ATPase domain of *Streptococcus pneumoniae* Topo IV indicate that the T-segment could be captured by and reside in the cavity of the N-gate (44). Our data show that gyrase can capture the complete DNA crossover, without needing to close the N-gate. At this step, the conformation of the ATPase domains appears to impede the binding of AMP-PNP at the active site (fig. S7, D and E). In addition, the position of the T-segment is presently incompatible with a dimerization of the ATPase domains in an upper position because of steric hindrance (fig. S6E). In the eukaryotic enzymes, the dimensions of the ATPase domain cavity would be unlikely to accommodate a DNA double helix (45), which suggests that simultaneous capture of a G- and T-segment, with an opened N-Gate, would be a favored mechanism for other TopoIIA.

After DNA crossover binding, N-gate closure could be triggered by the movement of the TOPRIM domain upon DNA cleavage and accompanying DNA gate opening. The TOPRIM domain could promote this upward movement of the ATP-binding domain by pulling on the linker of the transducer helices (fig. S2). In *E. coli* gyrase, the TOPRIM insertion could act as a “steric buttress” to promote communication between the functional domains, as previously mentioned (33). The insertion in *E. coli* gyrase maintains the ATP-binding monomers in a position facilitating their ascent across the TOPRIM domain. This positioning could in turn facilitate the closing of the N-gate, which may explain the high processivity of *E. coli* DNA gyrase for relaxation of (+)SC DNA in contrast to other TopoIIA, without an insertion in the TOPRIM domain (fig. S12) (46).

Structural basis for the sign-inversion mechanism of DNA gyrase

One of our most unexpected results is that a positive crossover was formed, even though the DNA substrate used was negatively supercoiled. Disruptions to base pairing caused by the negative supercoiling result in hyperflexible sites in the DNA (46, 47), which may facilitate the tight wrapping of the DNA around the CTD (47, 48). The use of supercoiled minicircles, coupled with the streptavidin immobilization strategy, probably explains why we were able to capture a DNA crossover—direct evidence of DNA wrapping that has remained elusive for more than 40 years.

The first model trying to explain the supercoiling activity of DNA gyrase proposed the involvement of DNA wrapping (49). A second model based on a sign-inversion reaction was suggested to describe introduction of (−)SC by this enzyme (28). This model proposed that the enzyme binds to a positive crossover followed by a DNA strand passage through a DNA double-strand break that results in a sign inversion. Our results bring together the two models (fig. S13): DNA wrapping is the first crucial step for negative supercoiling, which is achieved by the inversion of the stabilized positive node.

Supplementary Material

Refer to Web version on PubMed Central for supplementary material.

ACKNOWLEDGMENTS

We thank L. Haas and V. Vidmar for technical assistance with minicircle preparation, A. Durand for his help with EM data collection, T. Strick for his help with magnetic tweezer experiments, and L. Bonnefond for his help with structure analysis. The authors acknowledge the High Performance Computing Center of the University of Strasbourg for supporting this work by providing scientific support and access to computing resources.

Funding:

This work was supported by the Agence Nationale de la Recherche grant ANR-19-CE11- 0001-01 to V.L. and M.N., and ANR-21-CE11-0040-01 to V.L.; L.Z. and J.M.F. were supported by funding from National Institutes of Health grant R35 GM141793 (to L.Z.). This work was supported by the Region Grand-Est, project 19-GE9-039, to V.L. and M.V, and by the Ligue Nationale Contre le Cancer to M.N. (“Equipe labellisée” program). This work used the Integrated Structural Biology platform of the Strasbourg Instruct-ERIC center IGBMC-CBI supported by FRISBI (ANR-10-INBS-0005) and EquipEx+ France Cryo-EM (ANR-21-ESRE-0046). This work of the Interdisciplinary Thematic Institute IMCBio+, as part of the ITI 2021-2028 program of the University of Strasbourg, CNRS, and INSERM, was supported by IdEx Unistra (ANR-10-IDEX-0002), and by SFRI-STRAT’US project (ANR-20-SFRI-0012) and EUR IMCBio (ANR-17-EURE-0023) under the framework of the France 2030 Program. B.L.D. is a doctoral fellow supported by EUR IMCBio funds. L.Y. is a doctoral fellow supported by the China Scholarship Council.

Data and materials availability:

All structural data and corresponding cryo-EM maps have been deposited to the PDB and EMDB under the accession codes pdb_00008qdx, EMD-18342, and EMD-18565 for the Gyrase/crossover complex; pdb_00008qqs and EMD-18603 for the Gyrase/linear DNA complex; and EMD-18605 and pdb_00008qqu for one monomer of Gyrase protein, EMD-18567 for the Gyrase pinwheel, and EMD-18566 for the Gyrase pinwheel/T-segment. Materials in the main text or the supplementary materials are available from V.L. upon reasonable request.

REFERENCES AND NOTES

1. Hatfield GW, Benham CJ, Annu. Rev. Genet 36, 175–203 (2002). [PubMed: 12429691]
2. Baranello L, Levens D, Gupta A, Kouzine F, Biochim. Biophys. Acta 1819, 632–638 (2012). [PubMed: 22233557]
3. Chong S, Chen C, Ge H, Xie XS, Cell 158, 314–326 (2014). [PubMed: 25036631]
4. Schoeffler AJ, Berger JM, Q. Rev. Biophys 41, 41–101 (2008). [PubMed: 18755053]
5. Butler MS et al., Antimicrob. Agents Chemother 66, e0199121 (2022). [PubMed: 35007139]
6. Delgado JL, Hsieh C-M, Chan N-L, Hiasa H, Biochem. J 475, 373–398 (2018). [PubMed: 29363591]
7. Adrian M et al., EMBO J. 9, 4551–4554 (1990). [PubMed: 2265618]
8. Cherny DI, Jovin TM, J. Mol. Biol 313, 295–307 (2001). [PubMed: 11800558]
9. Irobalieva RN et al., Nat. Commun 6, 8440 (2015). [PubMed: 26455586]
10. Pyne ALB et al., Nat. Commun 12, 1053 (2021). [PubMed: 33594049]
11. Zechiedrich EL, Osheroff N, EMBO J. 9, 4555–4562 (1990). [PubMed: 2176156]
12. Deibler RW, Mann JK, Sumners WL, Zechiedrich L, BMC Mol. Biol 8, 44 (2007). [PubMed: 17531098]
13. Buck GR, Zechiedrich EL, J. Mol. Biol 340, 933–939 (2004). [PubMed: 15236957]
14. Timsit Y, Várnai P, PLOS ONE 5, e9326 (2010). [PubMed: 20174470]

15. Rybenkov VV, Ullsperger C, Vologodskii AV, Cozzarelli NR, Science 277, 690–693 (1997). [PubMed: 9235892]
16. Hanke A, Ziraldo R, Levene SD, Molecules 26, 3375 (2021). [PubMed: 34204901]
17. Schmidt BH, Osheroff N, Berger JM, Nat. Struct. Mol. Biol 19, 1147–1154 (2012). [PubMed: 23022727]
18. Vanden Broeck A, Lotz C, Ortiz J, Lamour V, Nat. Commun 10, 4935 (2019). [PubMed: 31666516]
19. Vanden Broeck A et al., Nat. Commun 12, 2962 (2021). [PubMed: 34016969]
20. Roca J, Wang JC, Cell 77, 609–616 (1994). [PubMed: 8187179]
21. McClendon AK, Rodriguez AC, Osheroff N, J. Biol. Chem 280, 39337–39345 (2005). [PubMed: 16188892]
22. Corbett KD, Schoeffler AJ, Thomsen ND, Berger JM, J. Mol. Biol 351, 545–561 (2005). [PubMed: 16023670]
23. Kampranis SC, Maxwell A, Proc. Natl. Acad. Sci. U.S.A 93, 14416–14421 (1996). [PubMed: 8962066]
24. Ruthenburg AJ, Graybosch DM, Huetsch JC, Verdine GL, J. Biol. Chem 280, 26177–26184 (2005). [PubMed: 15897198]
25. Gellert M, Mizuuchi K, O'Dea MH, Nash HA, Proc. Natl. Acad. Sci. U.S.A 73, 3872–3876 (1976). [PubMed: 186775]
26. Corbett KD, Shultzaberger RK, Berger JM, Proc. Natl. Acad. Sci. U.S.A 101, 7293–7298 (2004). [PubMed: 15123801]
27. Stelljes JT, Weidlich D, Gubaev A, Klostermeier D, Nucleic Acids Res. 46, 6773–6784 (2018). [PubMed: 29893908]
28. Brown PO, Cozzarelli NR, Science 206, 1081–1083 (1979). [PubMed: 227059]
29. Singleton CK, Wells RD, Anal. Biochem 122, 253–257 (1982). [PubMed: 6287878]
30. Marechal N, Serrano BP, Zhang X, Weitz CJ, Nat. Commun 13, 2380 (2022). [PubMed: 35501346]
31. Bax BD et al., Nature 466, 935–940 (2010). [PubMed: 20686482]
32. Dong KC, Berger JM, Nature 450, 1201–1205 (2007). [PubMed: 18097402]
33. Schoeffler AJ, May AP, Berger JM, Nucleic Acids Res. 38, 7830–7844 (2010). [PubMed: 20675723]
34. Papillon J et al., Nucleic Acids Res. 41, 7815–7827 (2013). [PubMed: 23804759]
35. Strick TR, Croquette V, Bensimon D, Nature 404, 901–904 (2000). [PubMed: 10786800]
36. Costenaro L, Grossmann JG, Ebel C, Maxwell A, Structure 13, 287–296 (2005). [PubMed: 15698572]
37. Lanz MA, Klostermeier D, Nucleic Acids Res. 40, 10893–10903 (2012). [PubMed: 22977179]
38. Hobson MJ, Bryant Z, Berger JM, Nucleic Acids Res. 48, 2035–2049 (2020). [PubMed: 31950157]
39. Caron PR, Watt P, Wang JC, Mol. Cell. Biol 14, 3197–3207 (1994). [PubMed: 8164675]
40. McClendon AK et al., Biochemistry 47, 13169–13178 (2008). [PubMed: 19053267]
41. Crisona NJ, Strick TR, Bensimon D, Croquette V, Cozzarelli NR, Genes Dev. 14, 2881–2892 (2000). [PubMed: 11090135]
42. Gubaev A, Klostermeier D, Proc. Natl. Acad. Sci. U.S.A 108, 14085–14090 (2011). [PubMed: 21817063]
43. Petrella S et al., Structure 27, 579–589.e5 (2019). [PubMed: 30744994]
44. Laponogov I et al., Nat. Commun 9, 2579 (2018). [PubMed: 29968711]
45. Wei H, Ruthenburg AJ, Bechis SK, Verdine GL, J. Biol. Chem 280, 37041–37047 (2005). [PubMed: 16100112]
46. Ashley RE et al., Nucleic Acids Res. 45, 9611–9624 (2017). [PubMed: 28934496]
47. Randall GL, Zechiedrich L, Pettitt BM, Nucleic Acids Res. 37, 5568–5577 (2009). [PubMed: 19586933]

48. Fogg JM, Judge AK, Stricker E, Chan HL, Zechiedrich L, Nat. Commun 12, 5683 (2021). [PubMed: 34584096]
49. Liu LF, Wang JC, Proc. Natl. Acad. Sci. U.S.A 75, 2098–2102 (1978). [PubMed: 276855]
50. Deweese JE, Osheroff MA, Osheroff N, Biochem. Mol. Biol. Educ 37, 2–10 (2008). [PubMed: 19225573]

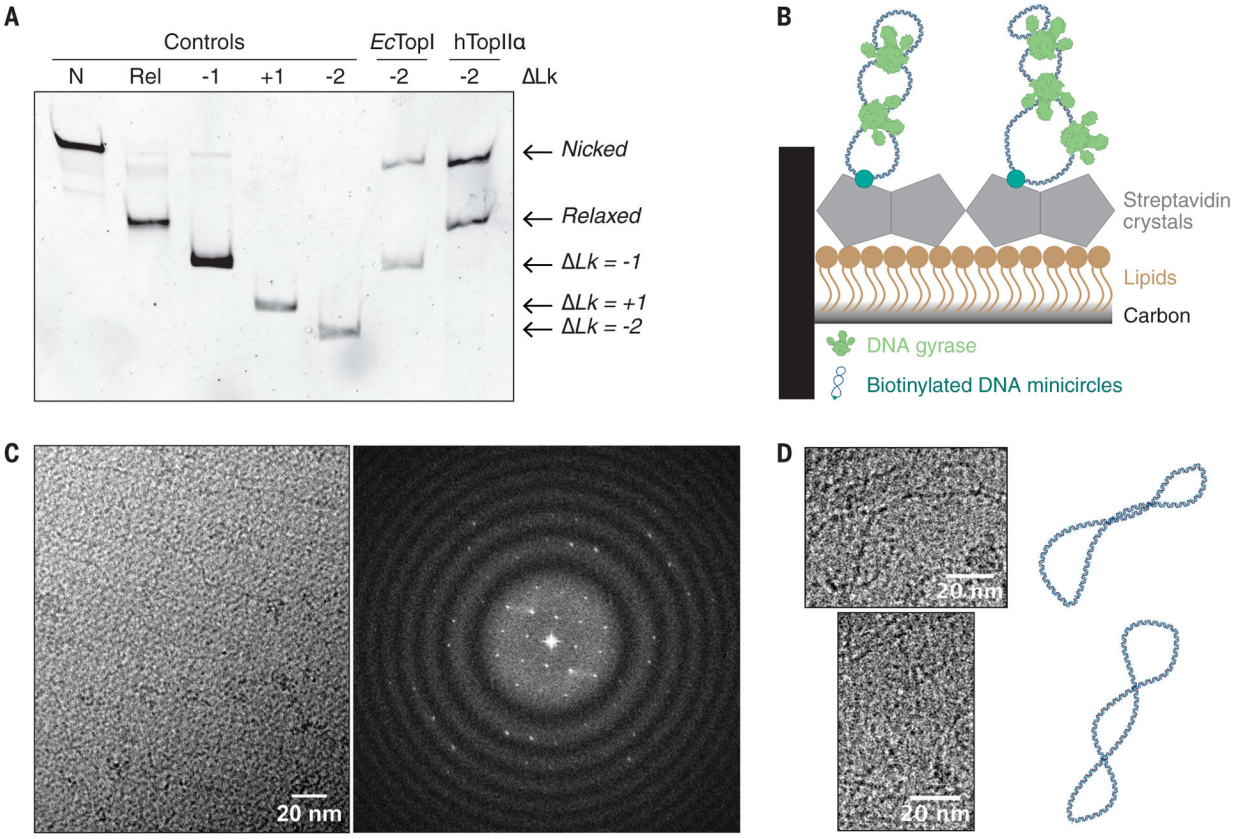

Fig. 1. DNA minicircle and cryo-EM strategy.

(A) Relaxation activities by type I (*Ec* Top1) and type II topoisomerases (hTopoIIα) of Δ*Lk* = −2 DNA minicircles. Controls are shown as N, nicked; Rel, relaxed; and Δ*Lk* = −1, +1, or −2 601-bp DNA minicircles. **(B)** Schematic representation of the SAG immobilizing the DNA minicircle–DNA gyrase complexes. **(C)** (Left) Cryo-EM micrograph and (right) power spectrum, with the diffraction pattern indicating the presence of 2D crystals. **(D)** Close-up on (Δ*Lk* = −2) SC DNA minicircles observed on micrographs after subtraction of the signal from the streptavidin crystals. Corresponding schematics of the DNA shapes are represented on the side.

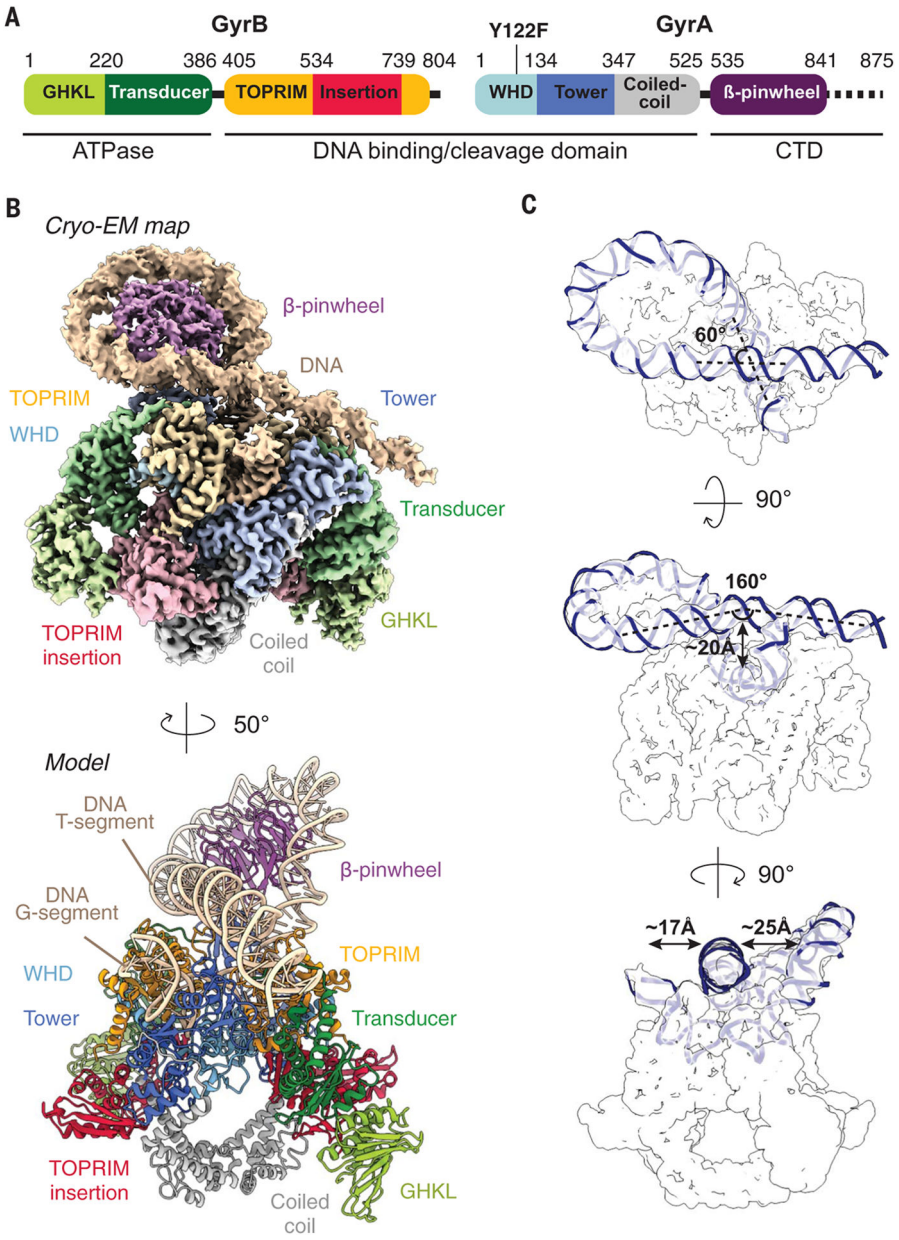

Fig. 2. Cryo-EM map and molecular model of *E. coli* DNA gyrase on a DNA crossover.

(A) Schematic representation of the GyrA and GyrB subdomains. The conserved catalytic tyrosine is located at position 122 in the GyrA subunit. The C-terminal tail of GyrA is indicated with a dotted line. **(B)** Cryo-EM composite map and molecular model of DNA gyrase bound to a DNA crossover (beige) with the same color coding as in (A) (movie S1). **(C)** T-segment orientation on DNA gyrase. The cryo-EM map of DNA gyrase is shown in outline, and the bound DNA crossover is rendered dark blue.

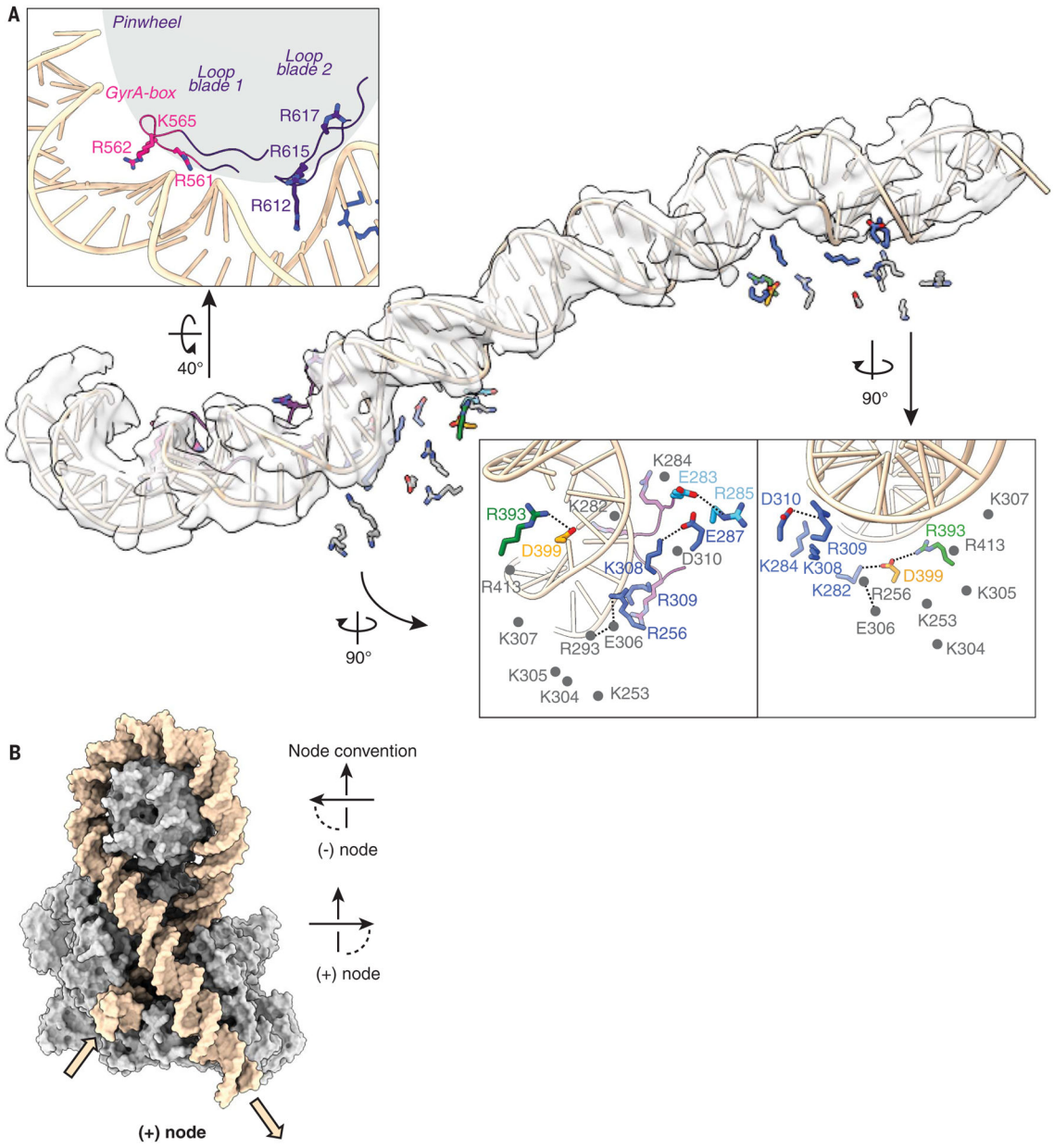

Fig. 3. DNA gyrase binds to a positive crossover.

(A) Molecular interactions around the T-segment. Conserved arginines in the β-pinwheel blade 1 "GyrA-box" and blade 2 are shown in pink and purple, respectively. The focused map around the T-segment (beige) appears as a white surface (local resolution, 4.2 Å). Residues decorating the surface of the groove belong to the Transducer/TOPRIM linker (green), TOPRIM domain (yellow), and Tower domain (dark blue). Depicted are positively charged residues and aspartic acids involved in hydrogen bond networks (dotted lines) at the beginning and end of the T-segment (gray), with residues also bridging the G-segment (cyan). **(B)** Surface representation of DNA gyrase bound to the positive DNA crossover and schematic representation of the DNA node sign convention (50). A DNA node or crossover is the point of contact of a strand of supercoiled DNA where it loops back on itself. The

geometry of the node (or crossover) can be of opposite chirality depending on the respective orientation of the 2 DNA molecules.

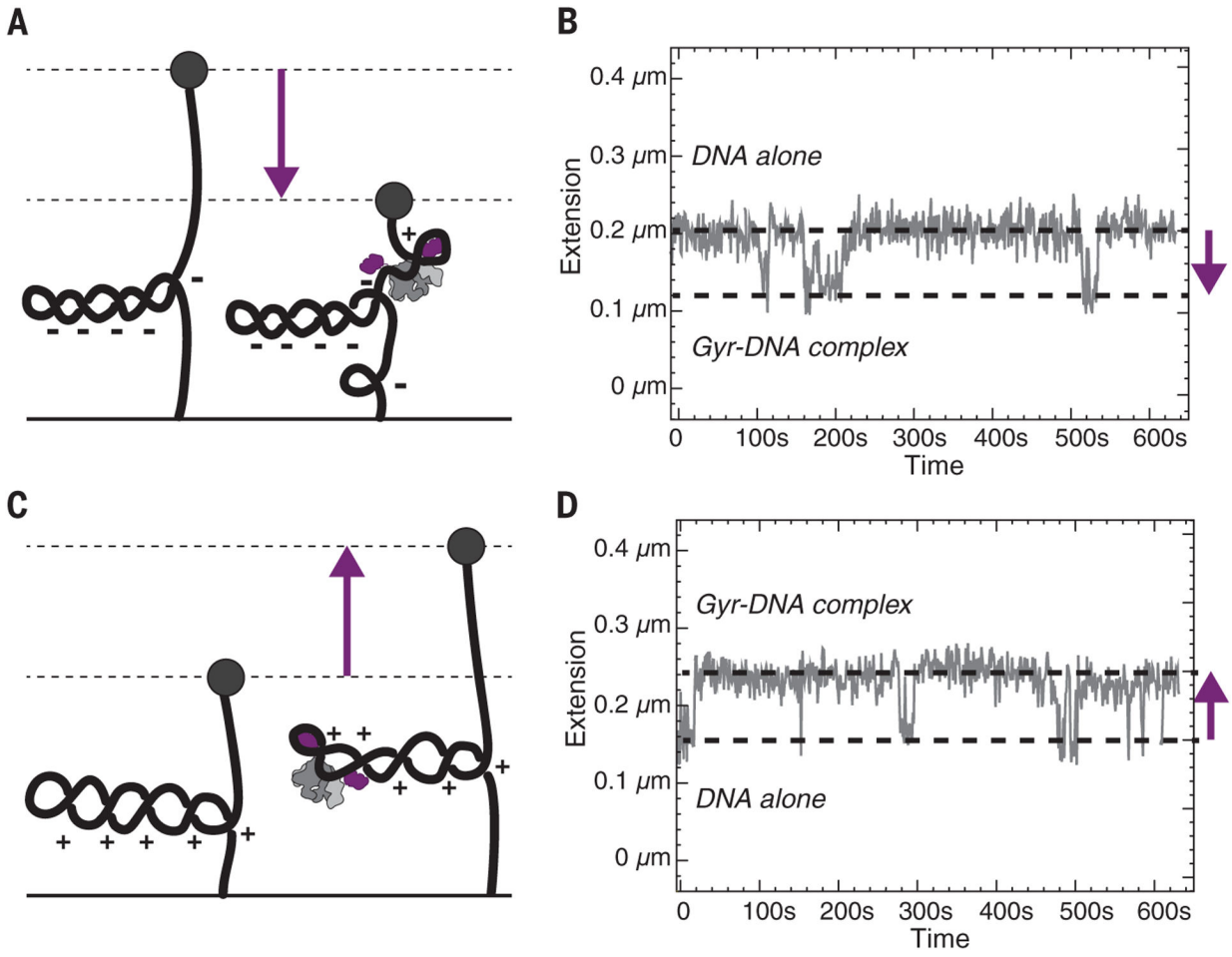

Fig. 4. Single-molecule assay of DNA gyrase binding to positively or negatively supercoiled DNA.

(**A** and **C**) Sketch of the experimental setup showing the DNA molecule tethered between a glass surface and a magnetic bead, which is manipulated by a magnetic trap. (A) Gyrase wraps DNA around a pinwheel by forming a positive supercoil. In compensation, an additional negative supercoil is formed in the rest of the molecule, reducing the DNA extension. (C) Upon binding to positive DNA supercoils, the DNA wraps around one pinwheel, resulting in the release of DNA relative to an unbound supercoil, which results in an increase of DNA extension. (**B** and **D**) Time trace for the extension of a DNA containing (B) five negative supercoils or (D) five positive supercoils in the presence of the gyrase catalytically inactive mutant and 10 μM ATP. The force applied on the magnetic bead is 0.4 pN.